

# Elastic properties of hidden order in URu<sub>2</sub>Si<sub>2</sub> are reproduced by a staggered nematic

Jaron Kent-Dobias , Michael Matty, and B. J. Ramshaw

Laboratory of Atomic and Solid State Physics, Cornell University, Ithaca, New York 14853, USA



(Received 21 January 2020; revised 3 July 2020; accepted 30 July 2020; published 20 August 2020)

We develop a phenomenological mean-field theory describing the hidden-order phase in URu<sub>2</sub>Si<sub>2</sub> as a nematic of the  $B_{1g}$  representation staggered along the  $c$  axis. Several experimental features are reproduced by this theory: the topology of the temperature-pressure phase diagram, the response of the elastic modulus  $(C_{11} - C_{12})/2$  above the transition at ambient pressure, and orthorhombic symmetry breaking in the high-pressure antiferromagnetic phase. In this scenario, hidden order is characterized by broken rotational symmetry that is modulated along the  $c$  axis, the primary order of the high-pressure phase is an unmodulated nematic, and the triple point joining those two phases with the high-temperature paramagnetic phase is a Lifshitz point.

DOI: [10.1103/PhysRevB.102.075129](https://doi.org/10.1103/PhysRevB.102.075129)

## I. INTRODUCTION

URu<sub>2</sub>Si<sub>2</sub> is a paradigmatic example of a material with an ordered state whose broken symmetry remains unknown. This state, known as *hidden order* (HO), sets the stage for unconventional superconductivity that emerges at even lower temperatures. At sufficiently large hydrostatic pressures, both superconductivity and HO give way to local moment antiferromagnetism (AFM) [1]. Modern theories [2–19] propose associating any of a variety of broken symmetries with HO. Motivated by the anomalous temperature dependence of one of the elastic moduli, this work analyzes a family of phenomenological models with order parameters of general symmetry that couple linearly to strain. Of these, only one is compatible with two experimental observations: first, the  $B_{1g}$  “nematic” elastic susceptibility  $(C_{11} - C_{12})/2$  softens anomalously from room temperature down to  $T_{HO} = 17.5$  K [20], and second, a  $B_{1g}$  nematic distortion is observed by x-ray scattering under sufficient pressure to destroy the HO state [21].

Recent resonant ultrasound spectroscopy (RUS) measurements were used to examine the thermodynamic discontinuities in the elastic moduli at  $T_{HO}$  [22]. The observation of discontinuities only in compressional, or  $A_{1g}$ , elastic moduli requires that the point-group representation of HO be one-dimensional. This rules out many order parameter candidates [11–15,19,23] in a model-independent way but does not differentiate between those that remain.

Recent x-ray experiments discovered rotational symmetry breaking in URu<sub>2</sub>Si<sub>2</sub> under pressure [21]. Above 0.13–0.5 GPa (depending on temperature), URu<sub>2</sub>Si<sub>2</sub> undergoes a  $B_{1g}$  nematic distortion, which might be related to the anomalous softening of the  $B_{1g}$  elastic modulus  $(C_{11} - C_{12})/2$  that occurs over a broad temperature range at zero pressure [24–26]. Motivated by these results—which hint at a  $B_{1g}$  strain susceptibility associated with the HO state—we construct a phenomenological mean-field theory for an arbitrary order parameter (OP) coupled to strain and then determine the effect

of its phase transitions on the elastic response in different symmetry channels.

We find that only one OP representation reproduces the anomalous  $B_{1g}$  elastic modulus, which softens in a Curie-Weiss-like manner from room temperature and then cusps at  $T_{HO}$ . That theory associates HO with a  $B_{1g}$  OP modulated along the  $c$  axis, the high-pressure state with uniform  $B_{1g}$  order, and the triple point between them with a Lifshitz point. In addition to the agreement with the ultrasound data across a broad temperature range, our model predicts uniform  $B_{1g}$  strain at high pressure—the same distortion that was recently seen in x-ray scattering experiments [21]. This work strongly motivates future ultrasound experiments under pressure approaching the Lifshitz point, which should find that the  $(C_{11} - C_{12})/2$  modulus diverges as the uniform  $B_{1g}$  strain of the high-pressure phase is approached.

## II. MODEL AND PHASE DIAGRAM

The point group of URu<sub>2</sub>Si<sub>2</sub> is  $D_{4h}$ , and any theory must locally respect this symmetry in the high-temperature phase. Our phenomenological free-energy density contains three parts: the elastic free energy, the OP, and the interaction between strain and OP. The most general quadratic free energy of the strain  $\epsilon$  is  $f_{\text{ELASTIC}} = C_{ijkl}^0 \epsilon_{ij} \epsilon_{kl}$  [27]. The form of the bare moduli tensor  $C^0$  is further restricted by symmetry [28]. Linear combinations of the six independent components of strain form five irreducible components of strain in  $D_{4h}$  as

$$\begin{aligned} \epsilon_{A_{1g},1} &= \epsilon_{11} + \epsilon_{22}, & \epsilon_{B_{1g}} &= \epsilon_{11} - \epsilon_{22}, & \epsilon_{A_{1g},2} &= \epsilon_{33}, \\ \epsilon_{B_{2g}} &= 2\epsilon_{12}, & \epsilon_{E_g} &= 2\{\epsilon_{11}, \epsilon_{22}\}. \end{aligned} \quad (1)$$

All quadratic combinations of these irreducible strains that transform like  $A_{1g}$  are included in the free energy,

$$f_{\text{ELASTIC}} = \frac{1}{2} \sum_{\mathbf{X}} C_{\mathbf{X},ij}^0 \epsilon_{\mathbf{X},i} \epsilon_{\mathbf{X},j}, \quad (2)$$

where the sum is over irreducible representations (irreps) of the point group and the bare elastic moduli  $C_X^0$  are

$$\begin{aligned} C_{A_{1g},11}^0 &= \frac{1}{2}(C_{1111}^0 + C_{1122}^0), & C_{B_{1g}}^0 &= \frac{1}{2}(C_{1111}^0 - C_{1122}^0), \\ C_{A_{1g},22}^0 &= C_{3333}^0, & C_{B_{2g}}^0 &= C_{1212}^0, & C_{A_{1g},12}^0 &= C_{1133}^0, \\ C_{E_g}^0 &= C_{1313}^0. \end{aligned} \quad (3)$$

The interaction between strain and an OP  $\eta$  depends on the point-group representation of  $\eta$ . If this representation is  $X$ , the most general coupling to linear order is

$$f_{\text{INT}} = -b^{(i)}\epsilon_X^{(i)}\eta. \quad (4)$$

Many high-order interactions are permitted, and in the Appendix another of the form  $\epsilon^2\eta^2$  is added to the following analysis. If there exists no component of strain that transforms like the representation  $X$  then there can be no linear coupling. The next-order coupling is linear in strain and quadratic in order parameter, and the effect of this coupling at a continuous phase transition is to produce a jump in the  $A_{1g}$  elastic moduli if  $\eta$  is single component [29–31] and jumps in other elastic moduli if it is multicomponent [22]. Because we are interested in physics that anticipates the phase transition—for instance, that the growing OP susceptibility is reflected directly in the elastic susceptibility—we will focus our attention on OPs that can produce linear couplings to strain. Looking at the components present in (1), this rules out all of the  $u$  representations (which are odd under inversion), the  $A_{2g}$  irrep, and all half-integer (spinor) representations.

If the OP transforms like  $A_{1g}$  (e.g., a fluctuation in valence number), odd terms are allowed in its free energy and without fine-tuning any transition will be first order and not continuous. Since the HO phase transition is second order [20], we will henceforth rule out  $A_{1g}$  OPs as well. For the OP representation  $X$  as any of those remaining— $B_{1g}$ ,  $B_{2g}$ , or  $E_g$ —the most general quadratic free-energy density is

$$f_{\text{OP}} = \frac{1}{2}[r\eta^2 + c_{\parallel}(\nabla_{\parallel}\eta)^2 + c_{\perp}(\nabla_{\perp}\eta)^2 + D_{\perp}(\nabla_{\perp}^2\eta)^2] + u\eta^4, \quad (5)$$

where  $\nabla_{\parallel} = \{\partial_1, \partial_2\}$  transforms like  $E_u$  and  $\nabla_{\perp} = \partial_3$  transforms like  $A_{2u}$ . Other quartic terms are allowed—especially many for an  $E_g$  OP—but we have included only those terms necessary for stability when either  $r$  or  $c_{\perp}$  becomes negative as a function of temperature. The full free-energy functional of  $\eta$  and  $\epsilon$  is

$$\begin{aligned} F[\eta, \epsilon] &= F_{\text{OP}}[\eta] + F_{\text{ELASTIC}}[\epsilon] + F_{\text{INT}}[\eta, \epsilon] \\ &= \int dx (f_{\text{OP}} + f_{\text{ELASTIC}} + f_{\text{INT}}). \end{aligned} \quad (6)$$

Rather than analyze this two-argument functional directly, we begin by tracing out the strain and studying the behavior of the OP alone. Later, we will invert this procedure and trace out the OP when we compute the effective elastic moduli. The only strain relevant to an OP of representation  $X$  at linear coupling is  $\epsilon_X$ , which can be traced out of the problem exactly in mean-field theory. Extremizing the functional (6) with respect to  $\epsilon_X$  gives

$$0 = \left. \frac{\delta F[\eta, \epsilon]}{\delta \epsilon_X(x)} \right|_{\epsilon=\epsilon_*} = C_X^0 \epsilon_X^*(x) - b\eta(x), \quad (7)$$

which in turn gives the strain field conditioned on the state of the OP field as  $\epsilon_X^*[\eta](x) = (b/C_X^0)\eta(x)$  at all spatial coordinates  $x$  and  $\epsilon_Y^*[\eta] = 0$  for all other irreps  $Y \neq X$ . Upon substitution into (6), the resulting single-argument free-energy functional  $F[\eta, \epsilon_*[\eta]]$  has a density identical to  $f_{\text{OP}}$  with the identification  $r \rightarrow \tilde{r} = r - b^2/2C_X^0$ .

With the strain traced out, (5) describes the theory of a Lifshitz point at  $\tilde{r} = c_{\perp} = 0$  [32,33]. The properties discussed in the remainder of this section can all be found in a standard text (e.g., [34]). For a one-component OP ( $B_{1g}$  or  $B_{2g}$ ) and positive  $c_{\parallel}$ , it is traditional to make the field ansatz  $\langle \eta(x) \rangle = \eta_* \cos(q_*x_3)$ . For  $\tilde{r} > 0$  and  $c_{\perp} > 0$  or  $\tilde{r} > c_{\perp}^2/4D_{\perp}$  and  $c_{\perp} < 0$ , the only stable solution is  $\eta_* = q_* = 0$ , and the system is unmodulated. For  $\tilde{r} < 0$  there are free-energy minima for  $q_* = 0$  and  $\eta_*^2 = -\tilde{r}/4u$ , and this system has uniform order of the OP representation, e.g.,  $B_{1g}$  or  $B_{2g}$ . For  $c_{\perp} < 0$  and  $\tilde{r} < c_{\perp}^2/4D_{\perp}$  there are free-energy minima for  $q_*^2 = -c_{\perp}/2D_{\perp}$  and

$$\eta_*^2 = \frac{c_{\perp}^2 - 4D_{\perp}\tilde{r}}{12D_{\perp}u} = \frac{\tilde{r}_c - \tilde{r}}{3u} = \frac{|\Delta\tilde{r}|}{3u}, \quad (8)$$

with  $\tilde{r}_c = c_{\perp}^2/4D_{\perp}$ , and the system has modulated order. The transition between the uniform and modulated orderings is first order for a one-component OP and occurs along the line  $c_{\perp} = -2\sqrt{-D_{\perp}\tilde{r}/5}$ .

For a two-component OP ( $E_g$ ) we must also allow a relative phase between the two components of the OP. In this case the uniform ordered phase is stable only for  $c_{\perp} > 0$ , and the modulated phase is now characterized by helical order with  $\langle \eta(x) \rangle = \eta_* \{\cos(q_*x_3), \sin(q_*x_3)\}$ . The uniform to modulated transition is now continuous. This does not reproduce the physics of URu<sub>2</sub>Si<sub>2</sub>, whose HO phase is bounded by a line of first-order transitions at high pressure, and so we will henceforth neglect the possibility of a multicomponent order parameter—consistent with earlier ultrasound measurements [22]. Schematic phase diagrams for both the one- and two-component models are shown in Fig. 1.

### III. SUSCEPTIBILITY AND ELASTIC MODULI

We will now derive the effective elastic tensor  $C$  that results from the coupling of strain to the OP. The ultimate result, found in (17), is that  $C_X$  differs from its bare value  $C_X^0$  only for the representation  $X$  of the OP. Moreover, this modulus does not vanish at the unmodulated to modulated transition—as it would if the transition were a  $q = 0$  phase transition—but instead ends in a cusp. In this section we start by computing the susceptibility of the OP at the unmodulated to modulated transition and then compute the elastic modulus for the same.

The susceptibility of a single-component ( $B_{1g}$  or  $B_{2g}$ ) OP is

$$\begin{aligned} \chi^{(-1)}(x, x') &= \left. \frac{\delta^2 F[\eta, \epsilon_*[\eta]]}{\delta \eta(x) \delta \eta(x')} \right|_{\eta=\langle \eta \rangle} \\ &= [\tilde{r} - c_{\parallel} \nabla_{\parallel}^2 - c_{\perp} \nabla_{\perp}^2 + D_{\perp} \nabla_{\perp}^4 + 12u(\eta(x))^2] \\ &\quad \times \delta(x - x'), \end{aligned} \quad (9)$$

where  $\{-1\}$  indicates a functional reciprocal defined as

$$\int dx'' \chi^{(-1)}(x, x'') \chi(x'', x') = \delta(x - x'). \quad (10)$$

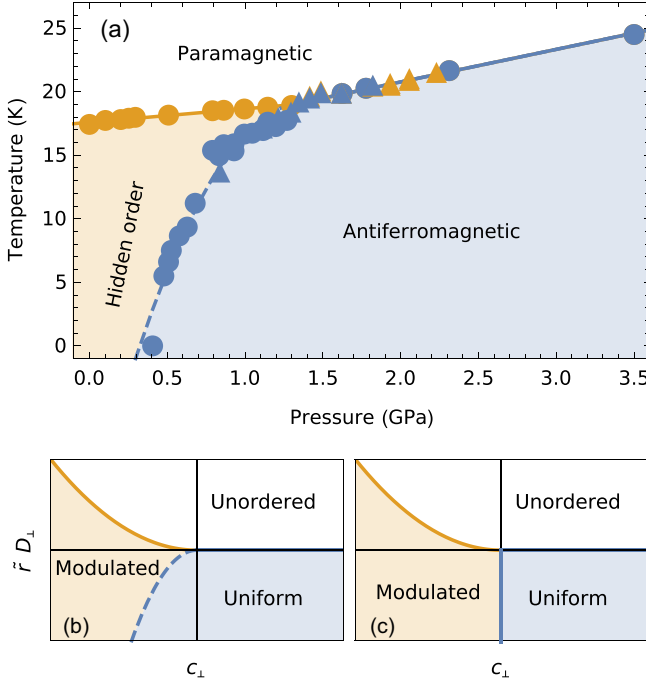


FIG. 1. Phase diagrams for (a) URu<sub>2</sub>Si<sub>2</sub> from experiments (neglecting the superconducting phase) [1], (b) mean-field theory of a one-component ( $B_{1g}$  or  $B_{2g}$ ) Lifshitz point, and (c) mean-field theory of a two-component ( $E_g$ ) Lifshitz point. Solid lines denote second-order transitions, while dashed lines denote first-order transitions. Later, when we fit the elastic moduli predictions for a  $B_{1g}$  OP to data along the ambient pressure line, we will take  $\Delta\tilde{r} = \tilde{r} - \tilde{r}_c = a(T - T_c)$ .

Taking the Fourier transform and integrating out  $q'$  give

$$\chi(q) = \left( \tilde{r} + c_{\parallel}q_{\parallel}^2 + c_{\perp}q_{\perp}^2 + D_{\perp}q_{\perp}^4 + 12u \sum_{q'} \langle \tilde{\eta}_{q'} \rangle \langle \tilde{\eta}_{-q'} \rangle \right)^{-1}. \quad (11)$$

Near the unordered to modulated transition this yields

$$\begin{aligned} \chi(q) &= [c_{\parallel}q_{\parallel}^2 + D_{\perp}(q_{\perp}^2 - q_{\perp}^2)^2 + |\Delta\tilde{r}|]^{-1} \\ &= \frac{1}{D_{\perp}} \frac{\xi_{\perp}^4}{1 + \xi_{\parallel}^2 q_{\parallel}^2 + \xi_{\perp}^4 (q_{\perp}^2 - q_{\perp}^2)^2}, \end{aligned} \quad (12)$$

with  $\xi_{\perp} = (|\Delta\tilde{r}|/D_{\perp})^{-1/4} = \xi_{\perp 0}|t|^{-1/4}$  and  $\xi_{\parallel} = (|\Delta\tilde{r}|/c_{\parallel})^{-1/2} = \xi_{\parallel 0}|t|^{-1/2}$ , where  $t = (T - T_c)/T_c$  is the reduced temperature and  $\xi_{\perp 0} = (D_{\perp}/aT_c)^{1/4}$  and  $\xi_{\parallel 0} = (c_{\parallel}/aT_c)^{1/2}$  are the bare correlation lengths perpendicular and parallel to the plane, respectively. The static susceptibility  $\chi(0) = (D_{\perp}q_{\perp}^4 + |\Delta\tilde{r}|)^{-1}$  does not diverge at the unordered to modulated transition. Although it anticipates a transition with Curie-Weiss-like divergence at the lower point  $a(T - T_c) = \Delta\tilde{r} = -D_{\perp}q_{\perp}^4 < 0$ , this is cut off with a cusp at the phase transition at  $\Delta\tilde{r} = 0$ .

The elastic susceptibility, which is the reciprocal of the effective elastic modulus, is found in a way similar to the OP susceptibility: we must trace over  $\eta$  and take the second variation of the resulting effective free-energy functional of  $\epsilon$  alone. Extremizing over  $\eta$  yields

$$0 = \left. \frac{\delta F[\eta, \epsilon]}{\delta \eta(x)} \right|_{\eta=\eta_{\star}} = \left. \frac{\delta F_{\text{OP}}[\eta]}{\delta \eta(x)} \right|_{\eta=\eta_{\star}} - b\epsilon_X(x), \quad (13)$$

which implicitly gives  $\eta_{\star}[\epsilon]$ , the OP conditioned on the configuration of the strain. Since  $\eta_{\star}$  is a functional of  $\epsilon_X$  alone, only the modulus  $C_X$  will be modified from its bare value  $C_X^0$ .

Although the differential equation for  $\eta_{\star}$  cannot be solved explicitly, we can use the inverse function theorem to make use of (13) anyway. First, denote by  $\eta_{\star}^{-1}[\eta]$  the inverse functional of  $\eta_{\star}$  implied by (13), which gives the function  $\epsilon_X$  corresponding to each solution of (13) it receives. This we can immediately identify from (13) as  $\eta_{\star}^{-1}[\eta](x) = b^{-1}\{\delta F_{\text{OP}}[\eta]/\delta \eta(x)\}$ . Now, we use the inverse function theorem to relate the functional reciprocal of the derivative of  $\eta_{\star}[\epsilon]$  with respect to  $\epsilon_X$  to the derivative of  $\eta_{\star}^{-1}[\eta]$  with respect to  $\eta$ , yielding

$$\begin{aligned} \left( \frac{\delta \eta_{\star}[\epsilon](x)}{\delta \epsilon_X(x')} \right)^{\{-1\}} &= \left. \frac{\delta \eta_{\star}^{-1}[\eta](x)}{\delta \eta(x')} \right|_{\eta=\eta_{\star}[\epsilon]} \\ &= b^{-1} \left. \frac{\delta^2 F_{\text{OP}}[\eta]}{\delta \eta(x)\delta \eta(x')} \right|_{\eta=\eta_{\star}[\epsilon]}. \end{aligned} \quad (14)$$

Next, (13) and (14) can be used in concert with the ordinary rules of functional calculus to yield the second variation

$$\begin{aligned} \frac{\delta^2 F[\eta_{\star}[\epsilon], \epsilon]}{\delta \epsilon_X(x)\delta \epsilon_X(x')} &= C_X^0 \delta(x - x') - 2b \frac{\delta \eta_{\star}[\epsilon](x)}{\delta \epsilon_X(x')} - b \int dx'' \frac{\delta^2 \eta_{\star}[\epsilon](x)}{\delta \epsilon_X(x')\delta \epsilon_X(x'')} \epsilon_X(x'') \\ &\quad + \int dx'' \frac{\delta^2 \eta_{\star}[\epsilon](x'')}{\delta \epsilon_X(x)\delta \epsilon_X(x')} \left. \frac{\delta F_{\text{OP}}[\eta]}{\delta \eta(x'')} \right|_{\eta=\eta_{\star}[\epsilon]} + \int dx'' dx''' \frac{\delta \eta_{\star}[\epsilon](x'')}{\delta \epsilon_X(x)} \frac{\delta \eta_{\star}[\epsilon](x''')}{\delta \epsilon_X(x')} \left. \frac{\delta^2 F_{\text{OP}}[\eta]}{\delta \eta(x'')\delta \eta(x''')} \right|_{\eta=\eta_{\star}[\epsilon]} \\ &= C_X^0 \delta(x - x') - 2b \frac{\delta \eta_{\star}[\epsilon](x)}{\delta \epsilon_X(x')} - b \int dx'' \frac{\delta^2 \eta_{\star}[\epsilon](x)}{\delta \epsilon_X(x')\delta \epsilon_X(x'')} \epsilon_X(x'') \\ &\quad + \int dx'' \frac{\delta^2 \eta_{\star}[\epsilon](x'')}{\delta \epsilon_X(x)\delta \epsilon_X(x')} [b\epsilon_X(x'')] + b \int dx'' dx''' \frac{\delta \eta_{\star}[\epsilon](x'')}{\delta \epsilon_X(x)} \frac{\delta \eta_{\star}[\epsilon](x''')}{\delta \epsilon_X(x')} \left( \frac{\partial \eta_{\star}[\epsilon](x'')}{\partial \epsilon_X(x''')} \right)^{\{-1\}} \\ &= C_X^0 \delta(x - x') - 2b \frac{\delta \eta_{\star}[\epsilon](x)}{\delta \epsilon_X(x')} + b \int dx'' \delta(x - x'') \frac{\delta \eta_{\star}[\epsilon](x'')}{\delta \epsilon_X(x')} = C_X^0 \delta(x - x') - b \frac{\delta \eta_{\star}[\epsilon](x)}{\delta \epsilon_X(x')}. \end{aligned} \quad (15)$$

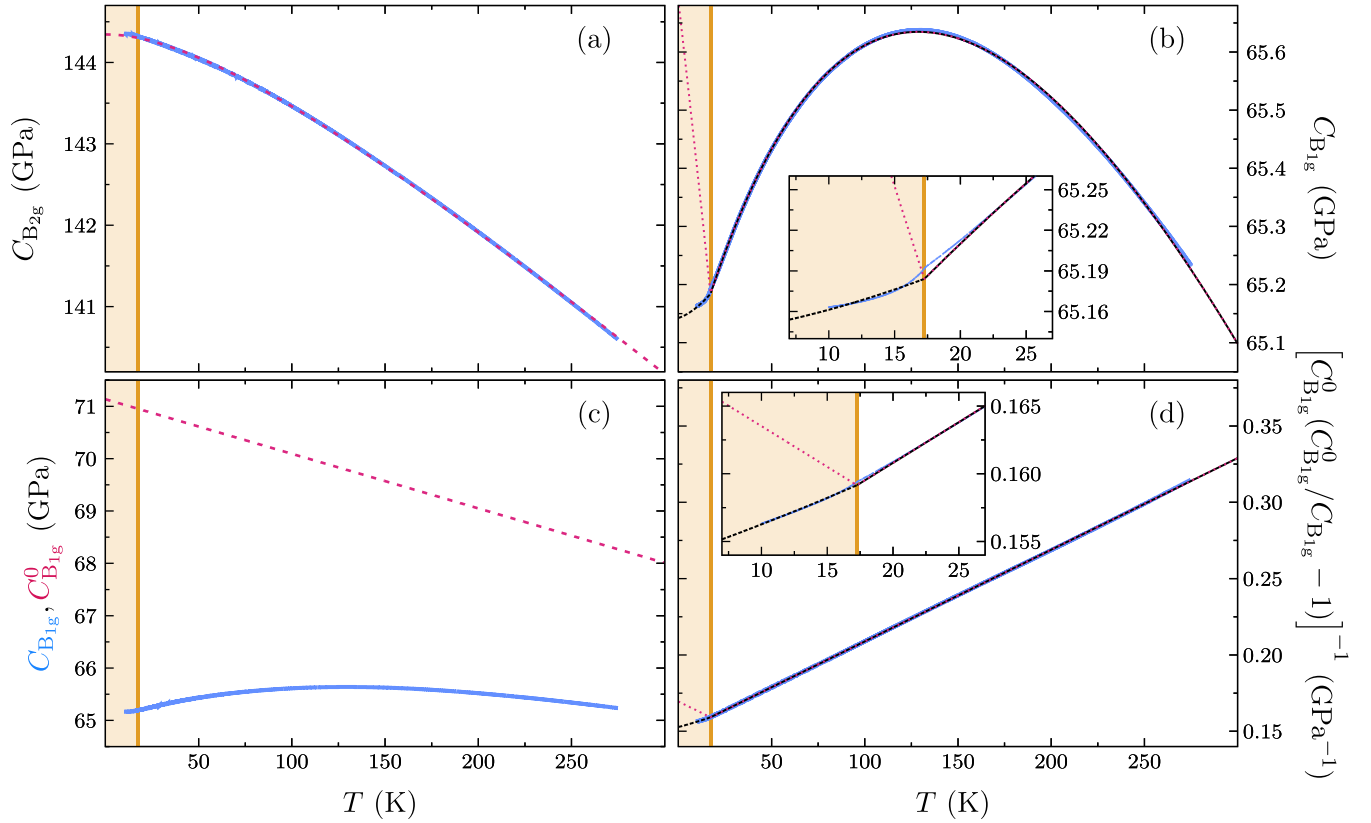


FIG. 2. RUS measurements of the elastic moduli of  $\text{URu}_2\text{Si}_2$  at ambient pressure as a function of temperature from recent experiments [22] (blue solid line) alongside fits to theory (magenta dashed and black dashed lines). The solid yellow region shows the location of the HO phase. (a)  $B_{2g}$  modulus data and a fit to the standard form [35]. (b)  $B_{1g}$  modulus data and a fit to (18) (magenta dashed line) and a fit to (A21) (black dashed line). The fit gives  $C_{B_{1g}}^0 \simeq [71 - (0.010 \text{ K}^{-1})T]$  GPa,  $b^2/D_{\perp}q_*^4 \simeq 6.28$  GPa, and  $b^2/a \simeq 1665$  GPa K $^{-1}$ . Addition of a quadratic term in  $C_{B_{1g}}^0$  was not needed here for the fit [35]. (c)  $B_{1g}$  modulus data and the fit of the bare  $B_{1g}$  modulus. (d)  $B_{1g}$  modulus data and the fits transformed by  $[C_{B_{1g}}^0 (C_{B_{1g}}^0 / C_{B_{1g}} - 1)]^{-1}$ , which is predicted from (18) to equal  $D_{\perp}q_*^4/b^2 + a/b^2|T - T_c|$ , e.g., an absolute-value function.

The elastic modulus is given by the second variation (15) evaluated at the extremized strain  $\langle \epsilon \rangle$ . To calculate it, note that evaluating the second variation of  $F_{\text{OP}}$  in (14) at  $\langle \epsilon \rangle$  (or  $\eta_*(\langle \epsilon \rangle) = \langle \eta \rangle$ ) yields

$$\left. \left( \frac{\delta \eta_*(\langle \epsilon \rangle(x))}{\delta \epsilon_X(x')} \right)^{\{-1\}} \right|_{\epsilon = \langle \epsilon \rangle} = b^{-1} \chi^{\{-1\}}(x, x') + \frac{b}{C_X^0} \delta(x - x'), \quad (16)$$

where  $\chi^{\{-1\}}$  is the OP susceptibility given by (9). Upon substitution into (15) and taking the Fourier transform of the result, we finally arrive at

$$C_X(q) = C_X^0 - b \left( \frac{1}{b\chi(q)} + \frac{b}{C_X^0} \right)^{-1} = C_X^0 \left( 1 + \frac{b^2}{C_X^0} \chi(q) \right)^{-1}. \quad (17)$$

Although not relevant here, this result generalizes to multi-component OPs.

What does (17) predict in the vicinity of the HO transition? Near the disordered-to-modulated transition—the zero-pressure transition to the HO state—the static modulus is given by

$$C_X(0) = C_X^0 \left[ 1 + \frac{b^2}{C_X^0} (D_{\perp}q_*^4 + |\Delta\tilde{r}|)^{-1} \right]^{-1}. \quad (18)$$

This corresponds to a softening in the  $X$  modulus approaching the transition that is cut off with a cusp of the form  $|\Delta\tilde{r}|^{\gamma} \propto |T - T_c|^{\gamma}$ , with  $\gamma = 1$ . This is our main result. The only OP irreps that couple linearly with strain and reproduce the topology of the  $\text{URu}_2\text{Si}_2$  phase diagram are  $B_{1g}$  and  $B_{2g}$ . For either of these irreps, the transition into a modulated rather than uniform phase masks traditional signatures of a continuous transition by locating thermodynamic singularities at nonzero  $q = q_*$ . The remaining clue at  $q = 0$  is a particular kink in the corresponding modulus.

#### IV. COMPARISON TO EXPERIMENT

RUS experiments [22] yield the individual elastic moduli broken into irreps; data for the  $B_{1g}$  and  $B_{2g}$  components defined in (1) are shown in Figs. 2(a) and 2(b). The  $B_{2g}$  modulus in Fig. 2(a) does not appear to have any response to the presence of the transition, exhibiting the expected linear stiffening upon cooling from room temperature, with a low-temperature cutoff at some fraction of the Debye temperature [35]. The  $B_{1g}$  modulus in Fig. 2(b) has a dramatic response, softening over the course of roughly 100 K and then cusping at the HO transition. The data in the high-temperature phase can be fit

to the theory (18), with a linear background modulus  $C_{B_{1g}}^0$  and  $\tilde{r} - \tilde{r}_c = a(T - T_c)$ , and the result is shown in Fig. 2(b).

The behavior of the modulus below the transition does not match (18) well, but this is because of the truncation of the free-energy expansion used above. Higher-order terms like  $\eta^2\epsilon^2$  and  $\epsilon^4$  contribute to the modulus starting at order  $\eta^2$  and therefore change the behavior below the transition, where the expectation value of  $\eta$  is finite, but not above it, where the expectation value of  $\eta$  is zero. To demonstrate this, in the Appendix we compute the modulus in a theory where the interaction free energy is truncated after fourth order with the new term  $\frac{1}{2}g\eta^2\epsilon^2$ . The dashed black line in Fig. 2 shows the fit of the RUS data to (A21) and shows that successive high-order corrections can account for the low-temperature behavior.

The data and theory appear quantitatively consistent, suggesting that HO can be described as a  $B_{1g}$ -nematic phase that is modulated at finite  $q$  along the  $c$  axis. The predicted softening appears over hundreds of kelvins; Figs. 2(c) and 2(d) show the background modulus  $C_{B_{1g}}^0$  and the OP-induced response isolated from each other.

We have seen that the mean-field theory of a  $B_{1g}$  OP recreates the topology of the HO phase diagram and the temperature dependence of the  $B_{1g}$  elastic modulus at zero pressure. This theory has several other physical implications. First, the association of a modulated  $B_{1g}$  order with the HO phase implies a *uniform*  $B_{1g}$  order associated with the high-pressure phase and, moreover, a uniform  $B_{1g}$  strain of magnitude  $(\epsilon_{B_{1g}})^2 = b^2\tilde{r}/4u(C_{B_{1g}}^0)^2$ , which corresponds to an orthorhombic structural phase. The onset of orthorhombic symmetry breaking was recently detected at high pressure in URu<sub>2</sub>Si<sub>2</sub> using x-ray diffraction, a further consistency of this theory with the phenomenology of URu<sub>2</sub>Si<sub>2</sub>[21].

Second, as the Lifshitz point is approached from low pressure, this theory predicts that the modulation wave vector  $q_*$  should vanish continuously. Far from the Lifshitz point we expect the wave vector to lock into values commensurate with the space group of the lattice and, moreover, that at zero pressure, where the RUS data here were collected, the half-wavelength of the modulation should be commensurate with the lattice spacing  $a_3 \simeq 9.68 \text{ \AA}$ , or  $q_* = \pi/a_3 \simeq 0.328 \text{ \AA}^{-1}$  [36–43]. In between these two regimes, mean-field theory predicts that the ordering wave vector shrinks by jumping between ever-closer commensurate values in the style of the devil's staircase [44]. In reality the presence of fluctuations may wash out these transitions.

This motivates future ultrasound experiments done under pressure, where the depth of the cusp in the  $B_{1g}$  modulus should deepen (perhaps with these commensurability jumps) at low pressure and approach zero as  $q_*^4 \sim (c_{\perp}/2D_{\perp})^2$  near the Lifshitz point. Alternatively, RUS done at ambient pressure might examine the heavy Fermi liquid to AFM transition by doping. Although previous RUS studies have doped URu<sub>2</sub>Si<sub>2</sub> with rhodium [45], rhodium changes the carrier concentration as well as the lattice spacing and may favor the promotion of the magnetic phase. An isoelectronic (as well as isomagnetic) dopant such as iron may more faithfully explore the transition out of the HO phase. Our work also motivates experiments that can probe the entire correlation function—like x-ray and neutron scattering—and directly resolve its finite-

$q$  divergence. The presence of spatial commensurability is known to be irrelevant to critical behavior at a one-component disordered-to-modulated transition and therefore is not expected to modify the thermodynamic behavior otherwise [46].

There are two apparent discrepancies between the orthorhombic strain in the phase diagram presented by recent x-ray data [21] and that predicted by our mean-field theory if its uniform  $B_{1g}$  phase is taken to be coincident with URu<sub>2</sub>Si<sub>2</sub>'s AFM. The first is the apparent onset of the orthorhombic phase in the HO state at slightly lower pressures than the onset of AFM. As recent x-ray research [21] notes, this misalignment of the two transitions as a function of doping could be due to the lack of an ambient pressure calibration for the lattice constant. The second discrepancy is the onset of orthorhombicity at higher temperatures than the onset of AFM. We note that magnetic susceptibility data see no trace of another phase transition at these higher temperatures [47]. It is therefore possible that the high-temperature orthorhombic signature in x-ray scattering is not the result of a bulk thermodynamic phase but, instead, marks the onset of short-range correlations, as it does in the high- $T_c$  cuprates [48] (where the onset of the charge density wave correlations also lacks a thermodynamic phase transition).

Three dimensions is below the upper critical dimension  $4\frac{1}{2}$  of a one-component disordered-to-modulated transition, and so mean-field theory should break down sufficiently close to the critical point due to fluctuations at the Ginzburg temperature [49,50]. Magnetic phase transitions tend to have a Ginzburg temperature of order 1. Our fit above gives  $\xi_{\perp 0}q_* = (D_{\perp}q_*^4/aT_c)^{1/4} \simeq 2$ , which combined with the speculation of  $q_* \simeq \pi/a_3$  puts the bare correlation length  $\xi_{\perp 0}$  on the order of lattice constant, which is about what one would expect for a generic magnetic transition. The agreement of these data in the  $(T - T_{HO})/T_{HO} \sim 0.1$ –10 range with the mean-field exponent suggests that this region is outside the Ginzburg region, but an experiment may begin to see deviations from mean-field behavior within approximately several kelvins of the critical point. An ultrasound experiment with finer temperature resolution near the critical point may be able to resolve a modified cusp exponent  $\gamma \simeq 1.31$  [51] since, according to one analysis, the universality class of a uniaxial modulated one-component OP is that of the O(2), three-dimensional XY transition [46]. A crossover from mean-field theory may explain the small discrepancy in our fit very close to the critical point.

## V. CONCLUSION AND OUTLOOK

We have developed a general phenomenological treatment of HO OPs that have the potential for linear coupling to strain. The two representations with mean-field phase diagrams that are consistent with the phase diagram of URu<sub>2</sub>Si<sub>2</sub> are  $B_{1g}$  and  $B_{2g}$ . Of these, only a staggered  $B_{1g}$  OP is consistent with zero-pressure RUS data, with a cusp appearing in the associated elastic modulus. In this picture, the HO phase is characterized by uniaxial modulated  $B_{1g}$  order, while the high-pressure phase is characterized by uniform  $B_{1g}$  order. The staggered nematic of HO is similar to the striped superconducting phase found in chemical compound lanthanum barium copper oxide and other cuprates [52].

We can also connect our results to the large body of work concerning various multipolar orders as candidate states for HO (e.g., Refs. [3–5,7–9]). Physically, our phenomenological order parameter could correspond to  $B_{1g}$  multipolar ordering originating from the localized component of the U  $5f$  electrons. For the crystal field states of  $\text{URu}_2\text{Si}_2$ , this could correspond either to electric quadrupolar or hexadecapolar order based on the available multipolar operators [4].

The coincidence of our theory's orthorhombic high-pressure phase and  $\text{URu}_2\text{Si}_2$ 's AFM is compelling, but our mean-field theory does not make any explicit connection with the physics of AFM. Neglecting this physics could be reasonable since correlations often lead to AFM as a secondary effect, like what occurs in many Mott insulators. An electronic theory of this phase diagram may find that the AFM observed in  $\text{URu}_2\text{Si}_2$  indeed follows along with an independent high-pressure orthorhombic phase associated with uniform  $B_{1g}$  electronic order.

The corresponding prediction of uniform  $B_{1g}$  symmetry breaking in the high-pressure phase is consistent with recent diffraction experiments [21], except for the apparent earlier onset in temperature of the  $B_{1g}$  symmetry breaking, which we believe may be due to fluctuating order at temperatures above the actual transition temperature. This work motivates both further theoretical work regarding a microscopic theory with modulated  $B_{1g}$  order and performing symmetry-sensitive thermodynamic experiments at pressure, such as pulse-echo ultrasound, that could further support or falsify this idea.

#### ACKNOWLEDGMENTS

J.K.-D. is supported by NSF Grant No. DMR-1719490, M.M. is supported by NSF Grant No. DMR-1719875, and B.J.R. is supported by NSF Grant No. DMR-1752784. We are grateful for helpful discussions with S. Raghu, S. Kivelson, D. Liarte, and J. Sethna and for permission to reproduce experimental data in our figure by E. Hassinger. We thank S. Ghosh for RUS data.

#### APPENDIX: ADDING A HIGHER-ORDER INTERACTION

In this Appendix, we compute the  $B_{1g}$  modulus for a theory with a high-order interaction truncation to better match the low-temperature behavior. Consider the free-energy density  $f = f_{\text{ELASTIC}} + f_{\text{INT}} + f_{\text{OP}}$ , with

$$f_{\text{ELASTIC}} = \frac{1}{2}C_0\epsilon^2, \quad f_{\text{INT}} = -b\epsilon\eta + \frac{1}{2}g\epsilon^2\eta^2, \quad f_{\text{OP}} = \frac{1}{2}[r\eta^2 + c_{\parallel}(\nabla_{\parallel}\eta)^2 + c_{\perp}(\nabla_{\perp}\eta)^2 + D(\nabla_{\perp}^2\eta)^2] + u\eta^4. \quad (\text{A1})$$

The mean-field strain conditioned on the order parameter is found from

$$\left. \frac{\delta F[\eta, \epsilon]}{\delta \epsilon(x)} \right|_{\epsilon=\epsilon_{\star}[\eta]} = C_0\epsilon_{\star}[\eta](x) - b\eta(x) + g\epsilon_{\star}[\eta](x)\eta(x)^2, \quad (\text{A2})$$

which yields

$$\epsilon_{\star}[\eta](x) = \frac{b\eta(x)}{C_0 + g\eta(x)^2}. \quad (\text{A3})$$

Upon substitution into (A1) and expanded to fourth order in  $\eta$ ,  $F[\eta, \epsilon_{\star}[\eta]]$  can be written in the form  $F_{\text{OP}}[\eta]$  alone with  $r \rightarrow \tilde{r} = r - b^2/C_0$  and  $u \rightarrow \tilde{u} = u + b^2g/2C_0^2$ . The phase diagram in  $\eta$  follows as before with the shifted coefficients, namely,  $\langle \eta(x) \rangle = \eta_{\star} \cos(q_{\star}x_3)$  for  $\tilde{r} < c_{\perp}^2/4D = \tilde{r}_c$ , with  $q_{\star}^2 = -c_{\perp}/2D$ , and

$$\eta_{\star}^2 = \frac{c_{\perp}^2 - 4D\tilde{r}}{12D\tilde{u}} = \frac{|\Delta\tilde{r}|}{3\tilde{u}}. \quad (\text{A4})$$

We would like to calculate the  $q$ -dependent modulus

$$C(q) = \frac{1}{V} \int dx dx' C(x, x') e^{-iq(x-x')}, \quad (\text{A5})$$

where

$$C(x, x') = \left. \frac{\delta^2 F[\eta_{\star}[\epsilon], \epsilon]}{\delta \epsilon(x)\delta \epsilon(x')} \right|_{\epsilon=\epsilon_{\star}[\eta_{\star}]} = \frac{\delta^2 F_{\text{ELASTIC}}[\eta_{\star}[\epsilon], \epsilon]}{\delta \epsilon(x)\delta \epsilon(x')} + \frac{\delta^2 F_{\text{INT}}[\eta_{\star}[\epsilon], \epsilon]}{\delta \epsilon(x)\delta \epsilon(x')} + \frac{\delta^2 F_{\text{OP}}[\eta_{\star}[\epsilon], \epsilon]}{\delta \epsilon(x)\delta \epsilon(x')} \Big|_{\epsilon=\epsilon_{\star}[\eta_{\star}]} \quad (\text{A6})$$

and  $\eta_{\star}$  is the mean-field order parameter conditioned on the strain defined implicitly by

$$0 = \left. \frac{\delta F[\eta, \epsilon]}{\delta \eta(x)} \right|_{\eta=\eta_{\star}[\epsilon]} = -b\epsilon(x) + g\epsilon(x)^2\eta_{\star}[\epsilon](x) + \frac{\delta F_{\text{OP}}[\eta]}{\delta \eta(x)} \Big|_{\eta=\eta_{\star}[\epsilon]}. \quad (\text{A7})$$

We will work this out term by term. The elastic term is the most straightforward, giving

$$\frac{\delta^2 F_{\text{ELASTIC}}[\epsilon]}{\delta \epsilon(x)\delta \epsilon(x')} = \frac{1}{2}C_0 \frac{\delta^2}{\delta \epsilon(x)\delta \epsilon(x')} \int dx'' \epsilon(x'')^2 = C_0\delta(x-x'). \quad (\text{A8})$$

The interaction term gives

$$\begin{aligned}
\frac{\delta^2 F_{\text{INT}}[\eta_\star[\epsilon], \epsilon]}{\delta\epsilon(x)\delta\epsilon(x')} &= -b \frac{\delta^2}{\delta\epsilon(x)\delta\epsilon(x')} \int dx'' \epsilon(x'') \eta_\star[\epsilon](x'') + \frac{1}{2} g \frac{\delta^2}{\delta\epsilon(x)\delta\epsilon(x')} \int dx'' \epsilon(x'')^2 \eta_\star[\epsilon](x'')^2 \\
&= -b \frac{\delta\eta_\star[\epsilon](x')}{\delta\epsilon(x)} - b \frac{\delta}{\delta\epsilon(x)} \int dx'' \epsilon(x'') \frac{\delta\eta_\star[\epsilon](x'')}{\delta\epsilon(x')} + g \frac{\delta}{\delta\epsilon(x)} \{\epsilon(x') \eta_\star[\epsilon](x')^2\} \\
&\quad + g \frac{\delta}{\delta\epsilon(x)} \int dx'' \epsilon(x'')^2 \eta_\star[\epsilon](x'') \frac{\delta\eta_\star[\epsilon](x'')}{\delta\epsilon(x')} \\
&= -2\{b - 2g\epsilon(x)\eta_\star[\epsilon](x)\} \frac{\delta\eta_\star[\epsilon](x)}{\delta\epsilon(x')} - b \int dx'' \epsilon(x'') \frac{\delta^2\eta_\star[\epsilon](x'')}{\delta\epsilon(x)\delta\epsilon(x')} + g\eta_\star[\epsilon](x)^2 \delta(x-x') \\
&\quad + g \int dx'' \epsilon(x'')^2 \frac{\delta\eta_\star[\epsilon](x'')}{\delta\epsilon(x)} \frac{\delta\eta_\star[\epsilon](x'')}{\delta\epsilon(x')} + g \int dx'' \epsilon(x'')^2 \eta_\star[\epsilon](x'') \frac{\delta^2\eta_\star[\epsilon](x'')}{\delta\epsilon(x)\delta\epsilon(x')}. \tag{A9}
\end{aligned}$$

The order parameter term relies on some other identities. First, (A7) implies

$$\left. \frac{\delta F_{\text{OP}}[\eta]}{\delta\eta(x)} \right|_{\eta=\eta_\star[\epsilon]} = b\epsilon(x) - g\epsilon(x)^2 \eta_\star[\epsilon](x) \tag{A10}$$

and therefore that the functional inverse  $\eta_\star^{-1}[\eta]$  is

$$\eta_\star^{-1}[\eta](x) = \frac{b}{2g\eta(x)} \left( 1 - \sqrt{1 - \frac{4g\eta(x)}{b^2} \frac{\delta F_{\text{OP}}[\eta]}{\delta\eta(x)}} \right). \tag{A11}$$

The inverse function theorem further implies [with substitution of (A10) after the derivative is evaluated] that

$$\left( \frac{\delta\eta_\star[\epsilon](x)}{\delta\epsilon(x')} \right)^{\{-1\}} = \left. \frac{\delta\eta_\star^{-1}[\eta](x)}{\delta\eta(x')} \right|_{\eta=\eta_\star[\epsilon]} = \frac{g\epsilon(x)^2 \delta(x-x') + \frac{\delta^2 F_{\text{OP}}[\eta]}{\delta\eta(x)\delta\eta(x')} \Big|_{\eta=\eta_\star[\epsilon]}}{b - 2g\epsilon(x)\eta_\star[\epsilon](x)} \tag{A12}$$

and therefore that

$$\left. \frac{\delta^2 F_{\text{OP}}[\eta]}{\delta\eta(x)\delta\eta(x')} \right|_{\eta=\eta_\star[\epsilon]} = \{b - 2g\epsilon(x)\eta_\star[\epsilon](x)\} \left( \frac{\delta\eta_\star[\epsilon](x)}{\delta\epsilon(x')} \right)^{\{-1\}} - g\epsilon(x)^2 \delta(x-x'). \tag{A13}$$

Finally, we evaluate the order parameter term, using (A10) and (A13), which give

$$\begin{aligned}
\frac{\delta^2 F_{\text{OP}}[\eta_\star[\epsilon]]}{\delta\epsilon(x)\delta\epsilon(x')} &= \frac{\delta}{\delta\epsilon(x)} \int dx'' \frac{\delta\eta_\star[\epsilon](x'')}{\delta\epsilon(x')} \left. \frac{\delta F_{\text{OP}}[\eta]}{\delta\eta(x'')} \right|_{\eta=\eta_\star[\epsilon]} \\
&= \int dx'' \frac{\delta^2\eta_\star[\epsilon](x'')}{\delta\epsilon(x)\delta\epsilon(x')} \left. \frac{\delta F_{\text{OP}}[\eta]}{\delta\eta(x'')} \right|_{\eta=\eta_\star[\epsilon]} + \int dx'' dx''' \frac{\delta\eta_\star[\epsilon](x'')}{\delta\epsilon(x)} \frac{\delta\eta_\star[\epsilon](x''')}{\delta\epsilon(x')} \left. \frac{\delta^2 F_{\text{OP}}[\eta]}{\delta\eta(x'')\delta\eta(x''')} \right|_{\eta=\eta_\star[\epsilon]} \\
&= \int dx'' \frac{\delta^2\eta_\star[\epsilon](x'')}{\delta\epsilon(x)\delta\epsilon(x')} \{b\epsilon(x) - g\epsilon(x)^2 \eta_\star[\epsilon](x)\} + \{b - 2g\epsilon(x)\eta_\star[\epsilon](x)\} \frac{\delta\eta_\star[\epsilon](x)}{\delta\epsilon(x')} \\
&\quad - g \int dx'' \epsilon(x'')^2 \frac{\delta\eta_\star[\epsilon](x'')}{\delta\epsilon(x)} \frac{\delta\eta_\star[\epsilon](x'')}{\delta\epsilon(x')}. \tag{A14}
\end{aligned}$$

Summing all three terms, we see a great deal of cancellation, with

$$\frac{\delta^2 F[\eta_\star[\epsilon], \epsilon]}{\delta\epsilon(x)\delta\epsilon(x')} = C_0 \delta(x-x') + g\eta_\star[\epsilon](x)^2 \delta(x-x') - \{b - 2g\epsilon(x)\eta_\star[\epsilon](x)\} \frac{\delta\eta_\star[\epsilon](x)}{\delta\epsilon(x')}.$$

We now need to evaluate this at  $\langle\epsilon\rangle$ . First,  $\eta_\star[\langle\epsilon\rangle] = \langle\eta\rangle$ , and

$$\left. \frac{\delta^2 F[\eta_\star[\epsilon], \epsilon]}{\delta\epsilon(x)\delta\epsilon(x')} \right|_{\epsilon=\langle\epsilon\rangle} = C_0 \delta(x-x') + g\langle\eta(x)\rangle^2 \delta(x-x') - [b - 2g\langle\epsilon(x)\rangle\langle\eta(x)\rangle] \left. \frac{\delta\eta_\star[\epsilon](x)}{\delta\epsilon(x')} \right|_{\epsilon=\langle\epsilon\rangle}.$$

Computing the final functional derivative is the most challenging part. We will first compute its functional inverse, take the Fourier transform of that, and then use the basic relationship between Fourier functional inverses to find the form of the noninverse. First, we note

$$\left. \frac{\delta^2 F_{\text{OP}}[\eta]}{\delta\eta(x)\delta\eta(x')} \right|_{\eta=\langle\eta\rangle} = [r - c_\perp \nabla_\perp^2 - c_\parallel \nabla_\parallel^2 + D \nabla_\perp^4 + 12u\langle\eta(x)\rangle^2] \delta(x-x'), \tag{A15}$$

which gives

$$\begin{aligned} \left. \left( \frac{\delta \eta_*[\epsilon](x)}{\delta \epsilon(x')} \right)^{\{-1\}} \right|_{\epsilon=\langle \epsilon \rangle} &= \frac{1}{b - 2g\langle \epsilon(x) \rangle \langle \eta(x) \rangle} \left[ g\langle \epsilon(x) \rangle^2 \delta(x-x') + \frac{\delta^2 F_{\text{OP}}[\eta]}{\delta \eta(x) \delta \eta(x')} \right]_{\eta=\langle \eta \rangle} \\ &= \frac{1}{b - 2g\langle \epsilon(x) \rangle \langle \eta(x) \rangle} \left[ g\langle \epsilon(x) \rangle^2 + r - c_{\perp} \nabla_{\perp}^2 - c_{\parallel} \nabla_{\parallel}^2 + D \nabla_{\perp}^4 + 12u \langle \eta(x) \rangle^2 \right] \delta(x-x'). \end{aligned} \quad (\text{A16})$$

Upon substitution of (A3) and expansion to quadratic order in  $\langle \eta(x) \rangle$ , we find

$$\begin{aligned} \left. \left( \frac{\delta \eta_*[\epsilon](x)}{\delta \epsilon(x')} \right)^{\{-1\}} \right|_{\epsilon=\langle \epsilon \rangle} &= \frac{1}{b} \left\{ r - c_{\perp} \nabla_{\perp}^2 - c_{\parallel} \nabla_{\parallel}^2 + D \nabla_{\perp}^4 \right. \\ &\quad \left. + \langle \eta(x) \rangle^2 \left[ 12u + \frac{b^2 g}{C_0^2} + \frac{2g}{C_0} (r - c_{\perp} \nabla_{\perp}^2 - c_{\parallel} \nabla_{\parallel}^2 + D \nabla_{\perp}^4) \right] + O(\langle \eta \rangle^4) \right\} \delta(x-x'). \end{aligned} \quad (\text{A17})$$

Defining  $\widehat{\langle \eta \rangle^2} = \int dq' \langle \hat{\eta}(q') \rangle \langle \hat{\eta}(-q') \rangle$ , its Fourier transform is then

$$\begin{aligned} G(q) &= \frac{1}{V} \int dx dx' e^{-iq(x-x')} \left. \left( \frac{\delta \eta_*[\epsilon](x)}{\delta \epsilon(x')} \right)^{\{-1\}} \right|_{\epsilon=\langle \epsilon \rangle} \\ &= \frac{1}{b} \left\{ r + c_{\perp} q_{\perp}^2 + c_{\parallel} q_{\parallel}^2 + D q_{\perp}^4 + \widehat{\langle \eta \rangle^2} \left[ 12u + \frac{b^2 g}{C_0^2} + \frac{2g}{C_0} (r + c_{\perp} q_{\perp}^2 + c_{\parallel} q_{\parallel}^2 + D q_{\perp}^4) \right] + O(\langle \hat{\eta} \rangle^4) \right\}. \end{aligned} \quad (\text{A18})$$

We can now compute  $C(q)$  by taking its Fourier transform, using the convolution theorem for the second term:

$$\begin{aligned} C(q) &= C_0 + g \widehat{\langle \eta \rangle^2} - \int dq' \left( b \delta(q'') - \frac{gb}{C_0} \int dq' \langle \hat{\eta}_{q'} \rangle \langle \hat{\eta}_{q''-q'} \rangle \right) / G(q-q'') \\ &= C_0 + g \widehat{\langle \eta \rangle^2} - b^2 \left( \frac{1}{r + c_{\perp} q_{\perp}^2 + c_{\parallel} q_{\parallel}^2 + D q_{\perp}^4} - \widehat{\langle \eta \rangle^2} \frac{12u + b^2 g/C_0^2 + \frac{2g}{C_0} (r + c_{\perp} q_{\perp}^2 + c_{\parallel} q_{\parallel}^2 + D q_{\perp}^4)}{(r + c_{\perp} q_{\perp}^2 + c_{\parallel} q_{\parallel}^2 + D q_{\perp}^4)^2} \right) \\ &\quad + \frac{gb^2}{C_0} \int dq' dq'' \frac{\langle \hat{\eta}_{q'} \rangle \langle \hat{\eta}_{q''-q'} \rangle}{r + c_{\perp} (q_{\perp} - q''_{\perp})^2 + c_{\parallel} (q_{\parallel} - q''_{\parallel})^2 + D (q_{\perp} - q''_{\perp})^4} + O(\langle \hat{\eta} \rangle^4). \end{aligned} \quad (\text{A19})$$

Upon substitution of  $\langle \hat{\eta}_q \rangle = \frac{1}{2} \eta_* [\delta(q_{\perp} - q_*) + \delta(q_{\perp} + q_*)] \delta(q_{\parallel})$ , we have

$$\begin{aligned} C(q) &= C_0 + \frac{1}{4} g \eta_*^2 - b^2 \left( \frac{1}{r + c_{\perp} q_{\perp}^2 + c_{\parallel} q_{\parallel}^2 + D q_{\perp}^4} - \frac{\eta_*^2}{4} \frac{12u + b^2 g/C_0^2 + \frac{2g}{C_0} (r + c_{\perp} q_{\perp}^2 + c_{\parallel} q_{\parallel}^2 + D q_{\perp}^4)}{(r + c_{\perp} q_{\perp}^2 + c_{\parallel} q_{\parallel}^2 + D q_{\perp}^4)^2} \right) \\ &\quad + \frac{gb^2 \eta_*^2}{4C_0} \left( \frac{2}{r + c_{\parallel} q_{\parallel}^2 + c_{\perp} q_{\perp}^2 + D q_{\perp}^4} + \frac{1}{r + c_{\parallel} q_{\parallel}^2 + c_{\perp} (q_{\perp} - 2q_*)^2 + D (q_{\perp} - 2q_*)^4} \right. \\ &\quad \left. + \frac{1}{r + c_{\parallel} q_{\parallel}^2 + c_{\perp} (q_{\perp} + 2q_*)^2 + D (q_{\perp} + 2q_*)^4} \right) + O(\eta_*^4). \end{aligned} \quad (\text{A20})$$

Evaluating at  $q = 0$ , we have

$$C(0) = C_0 - \frac{b^2}{r} + \frac{\eta_*^2}{4} \left( g + \frac{b^2}{r^2} (12u + b^2 g/C_0^2) + \frac{2gb^2}{C_0 r} \frac{16Dq_*^4 + 3r}{8Dq_*^4 + r} \right). \quad (\text{A21})$$

Above the transition this has exactly the form of (18) for any  $g$ ; below the transition it has the same form at  $g = 0$  to order  $\eta_*^2$ . With  $r = a\Delta T + c^2/4D + b^2/C_0$ ,  $u = \tilde{u} - b^2 g/2C_0^2$ , and

$$\eta_*^2 = \begin{cases} 0 & \Delta T > 0, \\ -a\Delta T/3\tilde{u} & \Delta T \leq 0, \end{cases} \quad (\text{A22})$$

we can fit the ratios  $b^2/a = 1665$  GPa K,  $b^2/Dq_*^4 = 6.28$  GPa, and  $b\sqrt{-g/\tilde{u}} = 14.58$  GPa with  $C_0 = [71.14 - (0.010426 \text{ K}^{-1})T]$  GPa. The resulting fit is shown as a dashed black line in Fig. 2.

[1] E. Hassinger, G. Knebel, K. Izawa, P. Lejay, B. Salce, and J. Flouquet, *Phys. Rev. B* **77**, 115117 (2008).

[2] S. Kambe, Y. Tokunaga, H. Sakai, T. Hattori, N. Higa, T. D. Matsuda, Y. Haga, R. E. Walstedt, and H. Harima, *Phys. Rev. B* **97**, 235142 (2018).

- [3] K. Haule and G. Kotliar, *Nat. Phys.* **5**, 796 (2009).
- [4] H. Kusunose and H. Harima, *J. Phys. Soc. Jpn.* **80**, 084702 (2011).
- [5] H.-H. Kung, R. E. Baumbach, E. D. Bauer, V. K. Thorsmølle, W.-L. Zhang, K. Haule, J. A. Mydosh, and G. Blumberg, *Science* **347**, 1339 (2015).
- [6] F. Cricchio, F. Bultmark, O. Grånäs, and L. Nordström, *Phys. Rev. Lett.* **103**, 107202 (2009).
- [7] F. J. Ohkawa and H. Shimizu, *J. Phys.* **11**, L519 (1999).
- [8] P. Santini and G. Amoretti, *Phys. Rev. Lett.* **73**, 1027 (1994).
- [9] A. Kiss and P. Fazekas, *Phys. Rev. B* **71**, 054415 (2005).
- [10] H. Harima, K. Miyake, and J. Flouquet, *J. Phys. Soc. Jpn.* **79**, 033705 (2010).
- [11] P. Thalmeier and T. Takimoto, *Phys. Rev. B* **83**, 165110 (2011).
- [12] S. Tonegawa, K. Hashimoto, K. Ikada, Y. H. Lin, H. Shishido, Y. Haga, T. D. Matsuda, E. Yamamoto, Y. Onuki, H. Ikeda, Y. Matsuda, and T. Shibauchi, *Phys. Rev. Lett.* **109**, 036401 (2012).
- [13] J. G. Rau and H.-Y. Kee, *Phys. Rev. B* **85**, 245112 (2012).
- [14] S. C. Riggs, M. C. Shapiro, A. V. Maharaj, S. Raghu, E. D. Bauer, R. E. Baumbach, P. Giraldo-Gallo, M. Wartenbe, and I. R. Fisher, *Nat. Commun.* **6**, 6425 (2015).
- [15] S. Hoshino, J. Otsuki, and Y. Kuramoto, *J. Phys. Soc. Jpn.* **82**, 044707 (2013).
- [16] H. Ikeda and Y. Ohashi, *Phys. Rev. Lett.* **81**, 3723 (1998).
- [17] P. Chandra, P. Coleman, and R. Flint, *Nature (London)* **493**, 621 (2013).
- [18] N. Harrison and M. Jaime, [arXiv:1902.06588](https://arxiv.org/abs/1902.06588).
- [19] H. Ikeda, M.-T. Suzuki, R. Arita, T. Takimoto, T. Shibauchi, and Y. Matsuda, *Nat. Phys.* **8**, 528 (2012).
- [20] A. de Visser, F. E. Kayzel, A. A. Menovsky, J. J. M. Franse, J. van den Berg, and G. J. Nieuwenhuys, *Phys. Rev. B* **34**, 8168 (1986).
- [21] J. Choi, O. Ivashko, N. Dennler, D. Aoki, K. von Arx, S. Gerber, O. Gutowski, M. H. Fischer, J. Strempfer, M. v. Zimmermann, and J. Chang, *Phys. Rev. B* **98**, 241113(R) (2018).
- [22] S. Ghosh, M. Matty, R. Baumbach, E. D. Bauer, K. A. Modic, A. Shekhter, J. A. Mydosh, E.-A. Kim, and B. J. Ramshaw, *Sci. Adv.* **6**, eaaz4074 (2020).
- [23] P. Chandra, P. Coleman, and R. Flint, *J. Phys.: Conf. Ser.* **449**, 012026 (2013).
- [24] B. Wolf, W. Sixl, R. Graf, D. Finsterbusch, G. Bruls, B. Lüthi, E. A. Knetsch, A. A. Menovsky, and J. A. Mydosh, *J. Low Temp. Phys.* **94**, 307 (1994).
- [25] T. Yanagisawa, S. Mombetsu, H. Hidaka, H. Amitsuka, M. Akatsu, S. Yasin, S. Zherlitsyn, J. Wosnitzer, K. Huang, and M. Brian Maple, *J. Phys. Soc. Jpn.* **82**, 013601 (2013).
- [26] K. Kuwahara, H. Amitsuka, T. Sakakibara, O. Suzuki, S. Nakamura, T. Goto, M. Mihalik, A. A. Menovsky, A. de Visser, and J. J. M. Franse, *J. Phys. Soc. Jpn.* **66**, 3251 (1997).
- [27] Components of the elastic modulus tensor  $C$  were given in the popular Voigt notation in the abstract and Introduction. Here and henceforth, the notation used is that natural for a rank-four tensor.
- [28] L. D. Landau, E. M. Lifshitz, A. M. Kosevich, and L. P. Pitaevskii, *Theory of elasticity*, 3rd ed., Landau and Lifshitz Course of Theoretical Physics, Vol. 7 (Pergamon Press, Oxford, 1986).
- [29] B. Lüthi and T. J. Moran, *Phys. Rev. B* **2**, 1211 (1970).
- [30] B. J. Ramshaw, A. Shekhter, R. D. McDonald, J. B. Betts, J. N. Mitchell, P. H. Tobash, C. H. Mielke, E. D. Bauer, and A. Migliori, *Proc. Natl. Acad. Sci. U.S.A.* **112**, 3285 (2015).
- [31] A. Shekhter, B. J. Ramshaw, R. Liang, W. N. Hardy, D. A. Bonn, F. F. Balakirev, R. D. McDonald, J. B. Betts, S. C. Riggs, and A. Migliori, *Nature (London)* **498**, 75 (2013).
- [32] E. M. Lifshitz, *Proc. USSR Acad. Sci. J. Phys.* **6**, 61 (1942).
- [33] E. M. Lifshitz, *Proc. USSR Acad. Sci. J. Phys.* **6**, 251 (1942).
- [34] P. M. Chaikin and T. C. Lubensky, *Principles of Condensed Matter Physics* (Cambridge University Press, Cambridge, 1995), Chap. 4, Sec. 6.5.
- [35] Y. P. Varshni, *Phys. Rev. B* **2**, 3952 (1970).
- [36] C. Bareille, F. L. Boariu, H. Schwab, P. Lejay, F. Reinert, and A. F. Santander-Syro, *Nat. Commun.* **5**, 4326 (2014).
- [37] R. Yoshida, Y. Nakamura, M. Fukui, Y. Haga, E. Yamamoto, Y. Onuki, M. Okawa, S. Shin, M. Hirai, Y. Muraoka, and T. Yokoya, *Phys. Rev. B* **82**, 205108 (2010).
- [38] R. Yoshida, K. Tsubota, T. Ishiga, M. Sunagawa, J. Sonoyama, D. Aoki, J. Flouquet, T. Wakita, Y. Muraoka, and T. Yokoya, *Sci. Rep.* **3**, 2750 (2013).
- [39] J.-Q. Meng, P. M. Oppeneer, J. A. Mydosh, P. S. Riseborough, K. Gofryk, J. J. Joyce, E. D. Bauer, Y. Li, and T. Durakiewicz, *Phys. Rev. Lett.* **111**, 127002 (2013).
- [40] C. Broholm, H. Lin, P. T. Matthews, T. E. Mason, W. J. L. Buyers, M. F. Collins, A. A. Menovsky, J. A. Mydosh, and J. K. Kjems, *Phys. Rev. B* **43**, 12809 (1991).
- [41] C. R. Wiebe, J. A. Janik, G. J. MacDougall, G. M. Luke, J. D. Garrett, H. D. Zhou, Y.-J. Jo, L. Balicas, Y. Qiu, J. R. D. Copley, Z. Yamani, and W. J. L. Buyers, *Nat. Phys.* **3**, 96 (2007).
- [42] F. Bourdarot, E. Hassinger, S. Raymond, D. Aoki, V. Taufour, L.-P. Regnault, and J. Flouquet, *J. Phys. Soc. Jpn.* **79**, 064719 (2010).
- [43] E. Hassinger, G. Knebel, T. D. Matsuda, D. Aoki, V. Taufour, and J. Flouquet, *Phys. Rev. Lett.* **105**, 216409 (2010).
- [44] P. Bak, *Rep. Prog. Phys.* **45**, 587 (1982).
- [45] T. Yanagisawa, *Philos. Mag.* **94**, 3775 (2014).
- [46] T. Garel and P. Pfeuty, *J. Phys. C* **9**, L245 (1976).
- [47] T. Inoue, K. Kindo, H. Okuni, K. Sugiyama, Y. Haga, E. Yamamoto, T. C. Kobayashi, Y. Uwatoko, and Y. Onuki, *Phys. B (Amsterdam, Neth.)* **294–295**, 271 (2001).
- [48] G. Ghiringhelli, M. Le Tacon, M. Minola, S. Blanco-Canosa, C. Mazzoli, N. B. Brookes, G. M. De Luca, A. Frano, D. G. Hawthorn, F. He, T. Loew, M. M. Sala, D. C. Peets, M. Salluzzo, E. Schierle, R. Sutarto, G. A. Sawatzky, E. Weschke, B. Keimer, and L. Braicovich, *Science* **337**, 821 (2012).
- [49] R. M. Hornreich, *J. Magn. Magn. Mater.* **15–18**, 387 (1980).
- [50] V. L. Ginzburg, *Fiz. Tverd. Tela* **2**, 2031 (1960) [*Sov. Phys. Solid State* **2**, 1824 (1961)].
- [51] R. Guida and J. Zinn-Justin, *J. Phys. A* **31**, 8103 (1998).
- [52] E. Berg, E. Fradkin, S. A. Kivelson, and J. M. Tranquada, *New J. Phys.* **11**, 115004 (2009).